

Rectangular Waveguide Diplexers With a Circular Waveguide Common Port

Tao Shen, *Associate Member, IEEE*, Kawthar A. Zaki, *Fellow, IEEE*, and Tim G. Dolan

Abstract—Design of rectangular waveguide diplexers with a circular waveguide common port is presented. Ridged *H*- and *E*-plane circular-to-rectangular-waveguide T-junctions are proposed as an optimum diplexing manifold. Full-wave optimization is used in the diplexer design. *Ka*-band *H*- and *E*-plane rectangular waveguide diplexers with a circular waveguide common port are designed. Measured results are in good agreement with computed results. The sensitivity of the diplexer performance with respect to the manufacturing tolerance is examined through tolerance analysis.

Index Terms—Waveguide diplexers.

I. INTRODUCTION

THE success of emerging *Ka*-band satellite systems for multimedia and broad-band high-speed Internet access is critically dependent on the availability of low-cost consumer terminals. Major cost drivers of these terminals are the RF/microwave subsystems and components. One of the most challenging components is the diplexer, which allows the use of a single antenna feed for both transmit and receive functions. The diplexer has stringent requirements on insertion loss, in-band flatness, selectivity, and rejection. For low-cost large-volume production, the diplexer must be designed to satisfy these stringent performance requirements and requires no manual tuning or adjustments after fabrication. In [1], the design of a *Ka*-band *H*-plane rectangular waveguide diplexer is described. In some applications, the common port of the diplexer must interface with a circular waveguide to be used in linear- or circular-polarization feed systems.

In this paper, design of rectangular waveguide diplexers with a circular waveguide common port is presented. Ridged *H*- and *E*-plane circular-to-rectangular-waveguide T-junctions are proposed as an optimum diplexing manifold. Full-wave optimization is used in the diplexer design. *Ka*-band *H*- and *E*-plane rectangular waveguide diplexers with a circular waveguide common port are designed. Measured results are in good agreement with computed results. The sensitivity of the diplexer performance with respect to the manufacturing tolerance is examined through tolerance analysis.

Manuscript received July 15, 2002.

T. Shen was with the Department of Electrical and Computer Engineering, University of Maryland at College Park, College Park, MD 20742 USA. He is now with the Hughes Network Systems, Germantown, MD 20876 USA (e-mail: tshen@hns.com).

K. A. Zaki is with the Department of Electrical and Computer Engineering, University of Maryland at College Park, College Park, MD 20742 USA (e-mail: zaki@eng.umd.edu).

T. G. Dolan is with the K&L Microwave Inc., Salisbury, MD 21804 USA. Digital Object Identifier 10.1109/TMTT.2002.807811

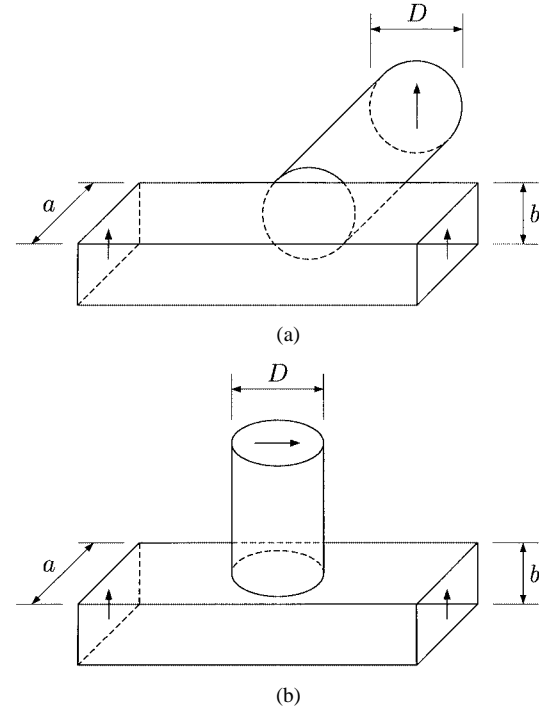
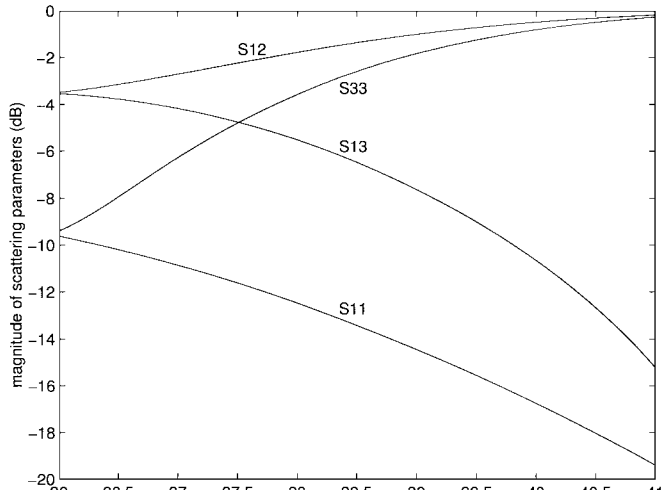


Fig. 1. Circular-to-rectangular-waveguide T-junctions. (a) *H*-plane. (b) *E*-plane.

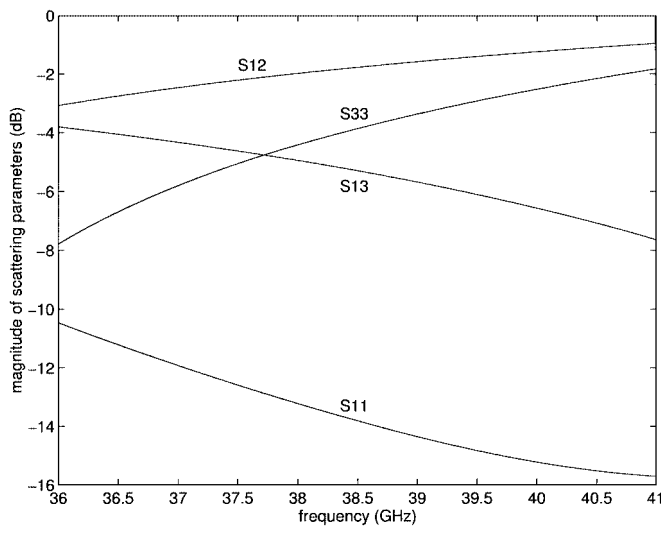
II. CIRCULAR-TO-RECTANGULAR-WAVEGUIDE T-JUNCTIONS

The dominant mode of the circular waveguide is the TE_{11} mode, having a cutoff wavelength $\lambda_c = 3.41D/2$ (D is the diameter of the circular waveguide). The TE_{11} mode is degenerate: two polarizations that are orthogonal to each other can propagate simultaneously. To ensure that only a single TE_{11} mode of the specified polarization can propagate, circular-to-rectangular-waveguide T-junctions should be configured properly such that the other polarization cannot be supported by the boundary conditions of the junctions [2]. Such configuration is shown in Fig. 1. For the *H*-plane T-junction, the junction structure should be symmetric with respect to the half- b -plane, which can be viewed as a perfect electric conductor (PEC). For the *E*-plane T-junction, the junction structure should be symmetric with respect to the half- a -plane, which can be viewed as a perfect magnetic conductor (PMC).

Fig. 2(a) and (b) shows the magnitudes of scattering parameters of the *H*- and *E*-plane T-junctions of Fig. 1, respectively, as a function of frequency. It has been proven [3] that the necessary conditions for an optimum three-port symmetric diplexing manifold are that the reflection coefficients of all three ports are approximately equal to or greater than $1/3$, and their dispersion over the frequency band covering channel filters is as



(a)



(b)

Fig. 2. Magnitudes of scattering parameters of the T-junctions of Fig. 1. (a) *H*-plane. (b) *E*-plane. Dimensions in inches are $a = 0.28$, $b = 0.14$, and $D = 0.21$. Ports 1 and 2 are of the rectangular waveguides and port 3 is of the circular waveguide.

small as possible. Here, it is found from the design experience that the so-called “optimum” does not necessarily mean that the “nonoptimum” T-junction cannot be used as a diplexing manifold under all circumstances. However, the “optimum” T-junction could facilitate the diplexer optimization process. It is seen from Fig. 2 that the scattering parameters of both *H*- and *E*-plane T-junctions of Fig. 1 are highly frequency dependent, and the magnitude of S_{11} is less than $1/3$ (-9.5 dB) for both T-junctions. Hence, the empty T-junctions of Fig. 1 are not suitable to be used as a diplexing manifold.

Instead, the ridged *H*- and *E*-plane circular-to-rectangular-waveguide T-junctions shown in Fig. 3 are proposed. By adjusting the ridge dimensions (w and s for the *H*-plane junction or h and s for the *E*-plane junction), optimum *H*- and *E*-plane T-junctions are obtained. Fig. 4 shows their magnitudes of scattering parameters as a function of frequency. It is seen that all scattering parameters are nearly frequency independent. For the *H*-plane T-junction, the magnitudes of

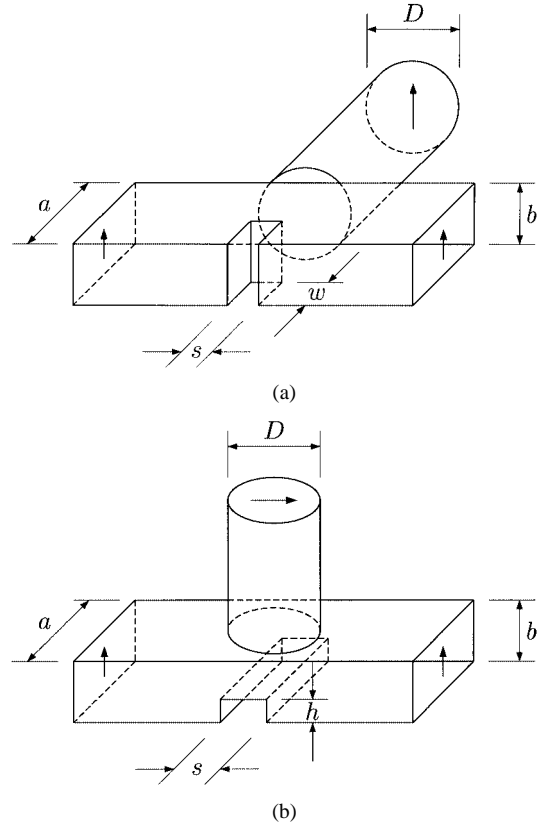


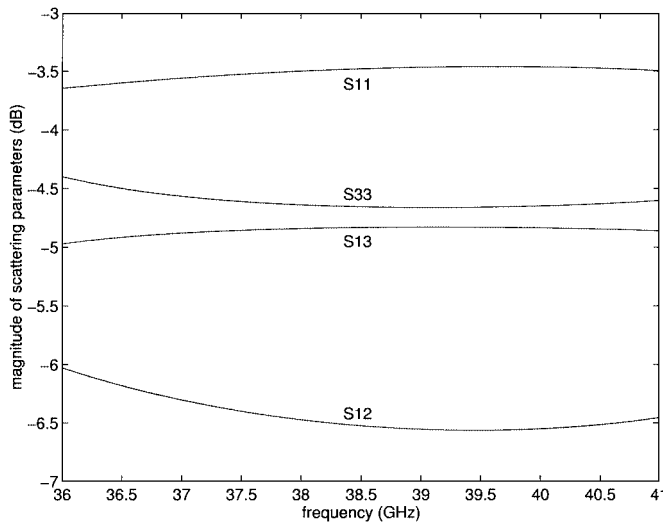
Fig. 3. Ridged circular-to-rectangular-waveguide T-junctions. (a) *H*-plane. (b) *E*-plane.

S_{11} and S_{33} are approximately equal to 0.67 (-3.5 dB) and 0.60 (-4.5 dB), respectively, over the whole frequency band, while for the *E*-plane T-junction, the magnitudes of S_{11} and S_{33} are approximately equal to 0.61 (-4.3 dB) and 0.35 (-9 dB), respectively, over the whole frequency band. Both *H*- and *E*-plane T-junctions satisfy the above-mentioned necessary conditions for an optimum diplexing manifold. In Section III, design examples of *Ka*-band *H*- and *E*-plane dippers using the above ridged circular-to-rectangular-waveguide T-junctions as a manifold will be presented.

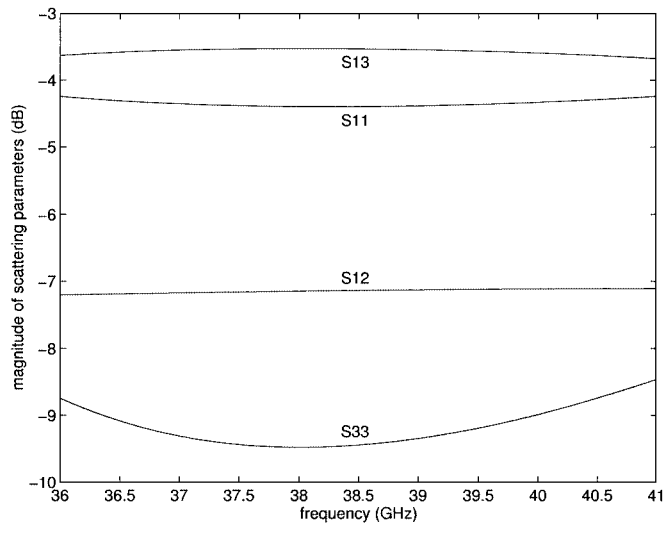
III. DIPLEXERS

Ka-band *H*- and *E*-plane rectangular waveguide dippers with a circular waveguide common port using the ridged T-junctions described in Section II are designed. The design specifications of the dippers are given in Tables I and II, and their configurations are shown in Fig. 5. In either *H*- or *E*-plane diplexer, both channel filters are of a six-cavity Chebyshev inductive-window type. In the modeling of the inductive-window direct-coupled channel filters, the rounded corner inherently introduced by the milling fabrication process is taken into account using step approximation [1]. This is necessary since, at *Ka*-band, the curvature radius of the rounded corner is of the order of the waveguide dimensions. Moreover, at *Ka*-band, the tuning screw is tiny and its dimensions are comparable with the waveguide dimensions too, which makes the post-fabrication tuning difficult.

A systematic optimization procedure is employed in the diplexer design [1], [4]. Two channel filters are designed



(a)



(b)

Fig. 4. Magnitudes of scattering parameters of the ridged T-junctions of Fig. 3. (a) *H*-plane. (b) *E*-plane. Dimensions in inches are $a = 0.28$, $b = 0.14$, and $D = 0.21$. For the *H*-plane T-junction, $w = 0.12$ and $s = 0.08$. For the *E*-plane T-junction, $h = 0.06$ and $s = 0.143$. Ports 1 and 2 are of the rectangular waveguides and port 3 is of the circular waveguide.

TABLE I
SPECIFICATION OF THE *H*-PLANE DIPLEXER

channel 1 passband	38.600 GHz to 38.950 GHz
channel 2 passband	39.300 GHz to 39.650 GHz
passband return loss	15 dB
passband insertion loss	2 dB
channel isolation	50 dB
channel 1 rejection	45 dB below 38.025 GHz
channel 2 rejection	45 dB above 40.225 GHz
temperature range	-33°C to +75°C

separately first, which are employed as the initial channel filters in the diplexer. The initial distances between the diplexing T-junction and channel filters could be determined according to [3]. In the diplexer optimization, the distances are optimized

TABLE II
SPECIFICATION OF THE *E*-PLANE DIPLEXER

channel 1 passband	37.058 GHz to 37.638 GHz
channel 2 passband	38.318 GHz to 38.898 GHz
passband return loss	15 dB
passband insertion loss	2 dB
channel isolation	50 dB
channel 1 rejection	45 dB below 36.598 GHz
channel 2 rejection	45 dB above 39.358 GHz
temperature range	-33°C to +75°C

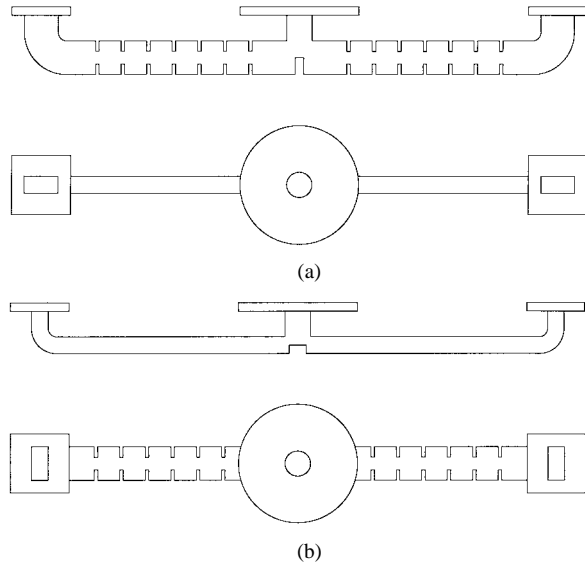


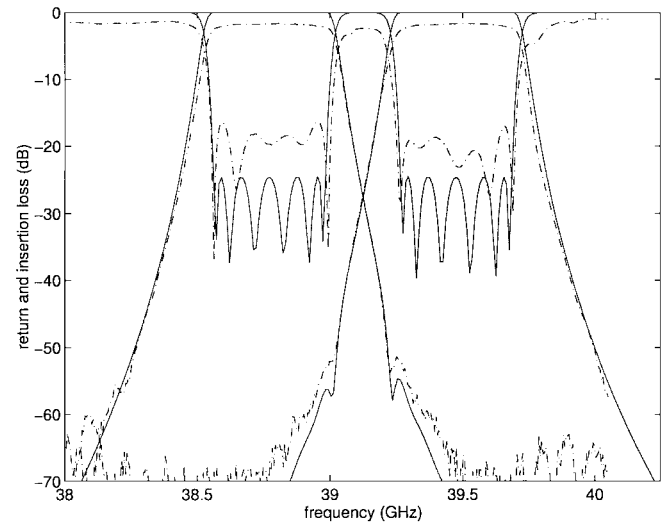
Fig. 5. Rectangular waveguide dippers with a circular waveguide common port. (a) *H*-plane. (b) *E*-plane.

first under a relatively loose diplexer specification. The channel filter dimensions are then included in the optimization from the first to last cavities successively under a progressively tighter diplexer specification. Finally, all diplexer dimensions are optimized under the exact diplexer specification.

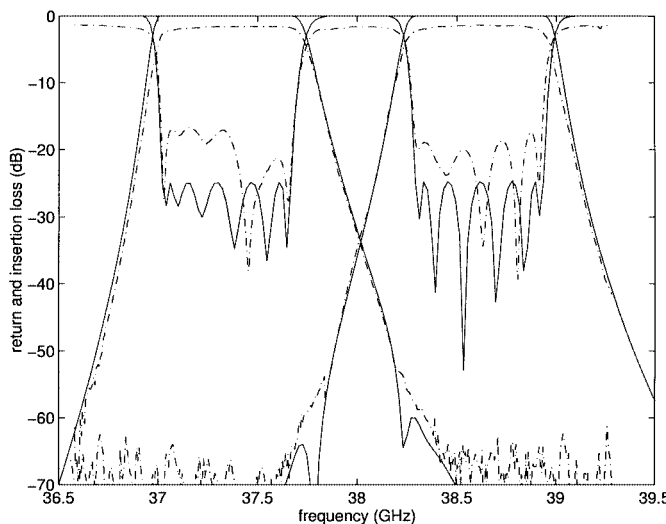
Fig. 6(a) and (b) shows the (computed and measured) responses of the *H*- and *E*-plane dippers, respectively. The measured results are in good agreement with the computed results, and the diplexer specification given in Tables I and II is achieved. There is a dip in the return-loss response of Fig. 6(a) next to the high-band channel approximately at 39.75 GHz. It is due to the imperfect transition between the circular waveguide and the rectangular waveguide test standard. The measurement of two back-to-back connected such transitions shows a dip at the same frequency. Note that, in order to satisfy the diplexer specification across the temperature range from -33°C to +75°C, the designed passband bandwidth of channel filters is 80 MHz wider than the specified one. In the filter design, the frequency shift ΔF due to the temperature variation ΔT could be estimated according to

$$\Delta F = \alpha f_0 \Delta T$$

where f_0 is the center frequency of the filter and α is the thermal expansion coefficient of the material. For example, $\alpha = 20 \times 10^{-6}$ (1/°C) for aluminum.



(a)



(b)

Fig. 6. Responses of the diplexers. (a) *H*-plane. (b) *E*-plane. The solid line is the computed response, while the dotted-dashed line is the measured response.

IV. TOLERANCE ANALYSIS

In practice, the sensitivity of the diplexer performance with respect to the manufacturing tolerance is critical in order to reduce the manufacturing cost and post-fabrication tuning efforts. This is especially important at millimeter waves (e.g., *Ka*-band) when low-cost large-volume production is involved. Through sensitivity analysis, it is found that the diplexer performance is more sensitive to the filter cavity length dimensions than to the other diplexer dimensions (inductive window widths, heights, thicknesses, and the distances between the diplexing T-junction and channel filters). Therefore, tight manufacturing tolerance should be imposed on the filter cavity length dimensions.

One way to characterize the effect of the manufacturing tolerance on the diplexer performance is Monte Carlo tolerance analysis, which reveals the effect of the random manufacturing tolerance on the diplexer performance. In Monte Carlo tolerance analysis, diplexer dimensions are varied randomly within a tolerance. For example, given a tolerance of ± 0.001 in, an inductive-window width of nominal value of 0.1 in could be any

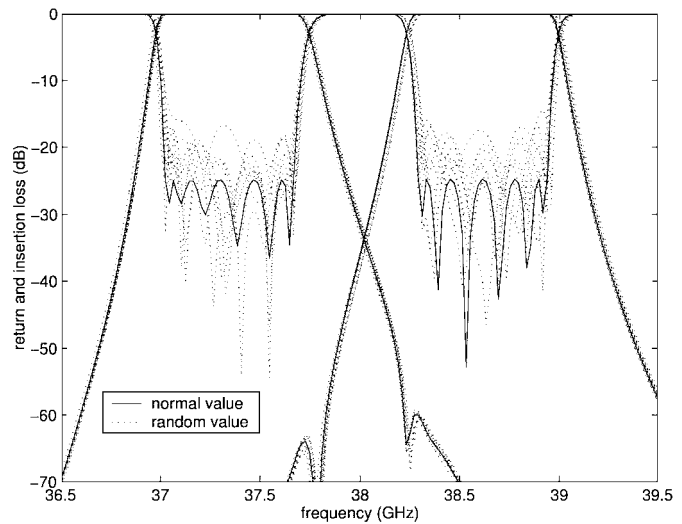


Fig. 7. Monte Carlo tolerance analysis of the *E*-plane diplexer. Tolerances of ± 0.1 mil and ± 0.2 mil are assumed for channel filter cavity length dimensions and other diplexer dimensions, respectively.

values between 0.099–0.101 in. Fig. 7 shows the Monte Carlo tolerance analysis of the *E*-plane diplexer. In computation, a tolerance of ± 0.1 mil for the filter cavity length dimensions is assumed, while a tolerance of ± 0.2 mil is assumed for other diplexer dimensions. In this figure, the solid line is the diplexer response computed using the nominal (optimized) dimensions, while the dotted line is the overlap of 15 diplexer responses computed using 15 sets of random dimensions. It is seen that the random manufacturing tolerance degrades the channel passband return loss, while it has nearly no effect on the channel isolation and rejection. Given the tolerances above, the diplexer response is kept well within the diplexer specification.

The other way to characterize the effect of the manufacturing tolerance on the diplexer performance is the worst case tolerance analysis, which reveals the effect of the uniform manufacturing tolerance on the diplexer performance. In the worst case tolerance analysis, diplexer dimensions are varied either at their max or min limits within a tolerance. For example, given a tolerance of ± 0.001 in, an inductive-window width of nominal value of 0.1 in could be either 0.099 or 0.101 in. Fig. 8 shows the worst case tolerance analysis of the *E*-plane diplexer. In computation, a tolerance of ± 0.5 mil is assumed for all diplexer dimensions. In this figure, the solid line is the diplexer response computed using the nominal dimensions, while the dotted line is the diplexer response computed using the dimensions 0.5 mil greater than nominal values, and the dashed line is the diplexer response computed using the dimensions 0.5 mil less than nominal values. It is seen that the diplexer response is intact, except that there is an approximate 50-MHz frequency shift. When the diplexer dimensions are increased by 0.5 mil, the response moves toward the low frequency end by 50 MHz. When diplexer dimensions are decreased by 0.5 mil, the response moves toward the high frequency end by 50 MHz.

Comparison of Figs. 7 and 8 shows that the uniform manufacturing tolerance has much less effect on the diplexer performance than the random manufacturing tolerance. Since

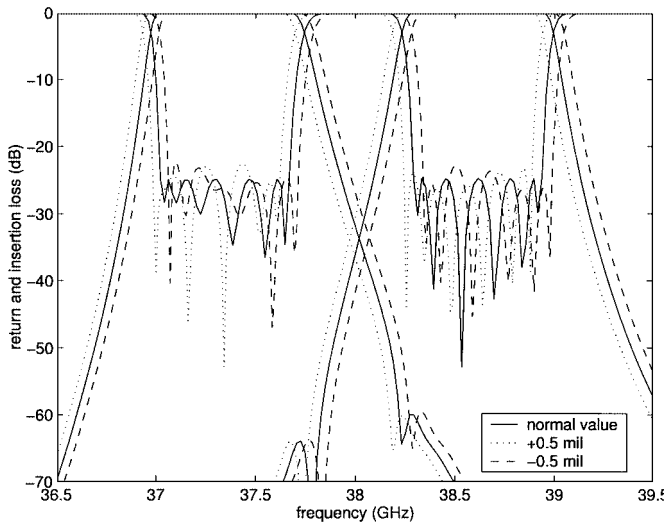


Fig. 8. Worst case tolerance analysis of the *E*-plane diplexer. A tolerance of ± 0.5 mil is assumed for all diplexer dimensions.

the practical fabrication process tends to minimize the random tolerance [5], a relatively loose manufacturing tolerance requirement could be expected.

V. SUMMARY

Design of rectangular waveguide dippers with a circular waveguide common port has been presented. Ridged *H*- and *E*-plane circular-to-rectangular-waveguide T-junctions have been proposed as an optimum diplexing manifold. Full-wave optimization has been used in the diplexer design. *Ka*-band *H*- and *E*-plane rectangular waveguide dippers with a circular waveguide common port have been designed. Measured results are in good agreement with computed results. The sensitivity of the diplexer performance with respect to the manufacturing tolerance has been examined through tolerance analysis. The uniform manufacturing tolerance has much less effect on the diplexer performance than the random manufacturing tolerance.

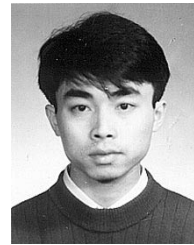
ACKNOWLEDGMENT

The authors would like to thank M. Smith, K&L Microwave Inc., Salisbury, MD, for providing measured data.

REFERENCES

[1] Y. Rong, H.-W. Yao, K. A. Zaki, and T. G. Dolan, "Millimeter-wave *Ka*-band *H*-plane dippers and multiplexers," *IEEE Trans. Microwave Theory Tech.*, vol. 47, pp. 2325-2330, Dec. 1999.

- [2] N. Marcuvitz, *Waveguide Handbook*. New York: McGraw-Hill, 1951.
- [3] A. Morini and T. Rozzi, "Constraints to the optimum performance and bandwidth limitations of dippers employing symmetric three-port junctions," *IEEE Trans. Microwave Theory Tech.*, vol. 44, pp. 242-248, Feb. 1996.
- [4] H.-W. Yao, A. E. Abdelmonem, J.-F. Liang, X.-P. Liang, K. A. Zaki, and A. Martin, "Wide-band waveguide and ridge waveguide T-junctions for diplexer applications," *IEEE Trans. Microwave Theory Tech.*, vol. 41, pp. 2166-2173, Dec. 1993.
- [5] Y.-C. Shih, "Manufacturing issues of millimeter-wave filters and dippers," presented at the IEEE MTT-S Comparative Filter Technologies for Communications Systems Workshop, Baltimore, MD, June 1998.



Tao Shen (S'95-A'01) was born in Suzhou, China, in 1969. He received the B.S. and M.S. degrees in radio engineering from Southeast University, Nanjing, China, in 1991 and 1994, respectively, and the Ph.D. degree in electrical and computer engineering from the University of Maryland at College Park, in 2001.

He is currently a Member of the Technical Staff with Hughes Network Systems, Germantown, MD. His research interests include characterization and development of RF and microwave components,

circuits, and subsystems.

Dr. Shen is on the Editorial Board of the *IEEE TRANSACTIONS ON MICROWAVE THEORY AND TECHNIQUES*.



Kawthar A. Zaki (SM'85-F'91) received the B.S. degree (with honors) from Ain Shams University, Cairo, Egypt, in 1962, and the M.S. and Ph.D. degrees from the University of California at Berkeley, in 1966 and 1969, respectively, all in electrical engineering.

From 1962 to 1964, she was a Lecturer in the Department of Electrical Engineering, Ain Shams University. From 1965 to 1969, she was a Research Assistant in the Electronics Research Laboratory, University of California at Berkeley. In 1970, she joined the Electrical Engineering Department, University of Maryland at College Park, where she is currently a Professor of electrical engineering. Her research interests are in the areas of electromagnetics, microwave circuits, simulation, optimization, and computer-aided design of advanced microwave and millimeter-wave systems and devices. She has authored or coauthored over 200 publications. She holds five patents on filters and dielectric resonators.

Prof. Zaki was the recipient of several academic honors and awards for teaching, research, and inventions.

Tim G. Dolan received the B.S. degree in electrical engineering from Pennsylvania State University, University Park, in 1982.

He possesses over 20 years experience in the electronics field. Since 1994, he has been with K&L Microwave Inc., Salisbury, MD, where he is currently the Vice President of Engineering. His responsibilities include research and development and corporate administration of the Engineering Department. He is also involved in the design of components and systems.